Published in final edited form as:
J Acquir Immune Defic Syndr. 2012 December 15; 61(5): 593–599. doi:10.1097/QAI.0b013e3182717c98.

Biphasic Elimination of Tenofovir Diphosphate and Nonlinear Pharmacokinetics of Zidovudine Triphosphate in a Microdosing Study

Jianmeng Chen[1], **Charles Flexner**[1], **Rosa G. Liberman**[2], **Paul L. Skipper**[2], **Nicolette Louissaint**[1], **Steven R. Tannenbaum**[2], **Craig Hendrix**[1], and **Edward Fuchs**[1]

[1]Division of Clinical Pharmacology, Johns Hopkins University School of Medicine, Baltimore, Maryland [2]Massachusetts Institute of Technology, Cambridge, MA

Abstract

Objective—Phase 0 studies can provide initial pharmacokinetics (PK) data in humans and help to facilitate early drug development, but their predictive value for standard dosing is controversial. To evaluate the prediction of microdosing for active intracellular drug metabolites, we compared the PK profile of two antiretroviral drugs, zidovudine (ZDV) and tenofovir (TFV), in microdose and standard dosing regimens.

Study Design—We administered a microdose (100 μg) of ^{14}C-labeled drug (ZDV or tenofovir disoproxil fumarate (TDF)) with or without a standard unlabelled dose (300 mg) to healthy volunteers. Both the parent drug in plasma and the active metabolite, ZDV-triphosphate (ZDV-TP) or TFV-diphosphate (TFV-DP) in PBMCs and CD4+ cells were measured by AMS.

Results—The intracellular ZDV-TP concentration increased less than proportionally over the dose range studied (100 μg to 300 mg), while the intracellular TFV-DP PK were linear over the same dose range. ZDV-TP concentrations were lower in CD4+ cells versus total peripheral blood mononuclear cells (PBMCs), while TFV-DP concentrations were not different in CD4+ cells and PBMCs.

Conclusion—Our data were consistent with a rate-limiting step in the intracellular phosphorylation of ZDV but not TFV. AMS shows promise for predicting the PK of active intracellular metabolites of nucleosides, but nonlinearity of PK may be seen with some drugs.

Keywords

Tenofovir diphosphate; Pharmacokinetics; Microdose

INTRODUCTION

The development of analytical techniques such as accelerator mass spectrometry (AMS) and highly sensitive LC-MS/MS allows assessment of bioavailability and plasma

Requests for reprints: Edward Fuchs, 600 N. Wolfe Street, Harvey 502, Baltimore, MD 21287. Phone 410-614-8762; Fax: 410-955-9708. ejfuchs@jhmi.edu.

Meetings Where Data Presented: "Use of Accelerator Mass Spectrometry (AMS) to Determine the Pharmacokinetic Profile of Intracellular Tenofovir Diphosphate (TFV-DP)" was presented at the 12th Int. Workshop on Clin. Pharmacology of HIV Therapy, April, 2011, Miami, FL.

Conflicts of Interest
The other authors have no competing financial interests.

pharmacokinetics (PK) in human subjects using a microdose (less than 100 μg) of drug [1–3]. Microdosing studies would allow early screening in human before extensive animal toxicity studies and GMP scale-up for phase I clinical studies to help identify the most promising drug candidates. It is not clear whether the kinetics of a microdose of a drug *in vivo* can predict the PK of a much larger therapeutic dose. However, there is mounting evidence that microdosing results are predictive of plasma PK and metabolism at the therapeutic dose level across a wide range of different chemical classes [4, 5].

The efficacy and toxicity of many human drugs depend on transport into target cells followed by conversion to an active or toxic metabolite. There are many nucleoside analog drugs whose efficacy depends on intracellular phosphorylation, including those used in anti-HIV treatment, viral hepatitis and cancer. Little is known about the PK of intracellular phosphorylation of these drugs in microdosing studies. In a previous trial, we have demonstrated that it is feasible to detect ^{14}C-labeled zidovudine triphosphate using AMS technology with high sensitivity, and we have successfully cross-validated these results using standard LC/MS/MS analysis [6]. With this technique we can thus directly compare the PK of intracellular phosphorylation in microdose and standard dose studies. Zidovudine (ZDV), a thymidine analog, and tenofovir (TFV), an adenosine analog, are nucleoside/nucleotide reverse transcriptase inhibitors (NRTI's) used in HIV treatment and prevention. These drugs are phosphorylated by different intracellular pathways [7, 8]. We used ^{14}C-labeled ZDV and ^{14}C-labeled tenofovir disoproxil fumarate (TDF) as model drugs to compare the PK of the active intracellular phosphorylated anabolite (ZDV-triphosphate, or ZDV-TP, and TFV-diphosphate, or TFV-DP), in total peripheral blood mononuclear cells (PBMC's) and isolated CD4+ T cells *in vivo* with both a microdose regimen and a standard dose regimen using AMS.

The PK of the active intracellular drug metabolite is important in evaluating the efficacy and toxicity of a drug and in choosing a dosing regimen. Evidence suggests that ZDV phosphorylation may be greatly reduced in CD4+ lymphocytes[9], which are the major target population for HIV infection, but no direct comparisons of TFV phosphorylation in T-cell subsets have been published. Here we directly compare TFV-DP and ZDV-TP measured in PBMCs and CD4+ T cells in subjects receiving a microdose or therapeutic dose of TDF.

METHODS

Subjects and study design

This protocol was reviewed and approved by the Johns Hopkins Medicine Institutional Review Board (IRB) and Radioactive Drug Review Committee (RDRC), and all subjects signed informed consent approved by the IRB. All subjects underwent a screening history and physical examination up to 28 days prior to participation. Enrolment criteria included age 18–55 years, normal renal function based on calculated creatinine clearance, hemoglobin >12 g/dL, HIV seronegative, and no medications or dietary supplements within 7 days prior to the study. No medications or supplements were allowed during the study.

This was a fixed-sequence study with two arms (ZDV arm and TDF arm). Six healthy subjects were enrolled for each arm. All twelve subjects received a microdose (20 μCi/100 μg) of ^{14}C labeled drug (ZDV or TDF) at first visit, and after a washout period of at least 30 days, all subjects received a standard dose (20 μCi/300.1 mg) of drug (ZDV or TDF). Detailed dosing information is described in supplemental Digital Content 1.

Chemicals and Materials

^{14}C-labeled ZDV [2-^{14}C-], ZDV-TP, and ^{14}C-labeled TDF [adenine-8-^{14}C-] were obtained from Moravek Biochemicals, Inc. (Brea, CA). HPLC-grade water and methanol were

purchased from VWR (Bridgeport, NJ). Analytical grade potassium chloride, sodium acetate, and acid phosphatase were acquired from Sigma-Aldrich Corp. (St Louis, MO). Waters XTerra^{R} MS C18 2.5 μm, 2.1×50mm columns, Waters Accell™ Plus QMA Cartridges, and Waters OASISR® HLB Extraction Cartridge were purchased from Waters Corporation (Milford, MA).

Sample collection and processing

PK samples for plasma, PBMC's and fractionated CD4+ T-lymphocytes were obtained predose, 2, 4, 8, 12, and 24 hours postdosing in the ZDV arm, and predose, 4, 12, 24, 72, and 168 hours postdosing in the TDF arm. At designated time points, 40 mL of blood was collected from each subject in CPT tubes (Becton, Dickinson and Company, Franklin Lakes, NJ) for the isolation of PBMCs. Two-thirds of the PBMCs were used to isolate CD4+ cells by MACS cell separation with CD4 microbeads and LS columns (Miltenyi Biotec, Bergisch Gladbach, Germany), as previously described [10]. Cells were washed and counted. 4 mL plasma was saved from the same samples for later PK analysis of parent drug concentrations.

For PBMC's and CD4+ cells obtained from 40 mL of blood, cells were counted and lysed as 10^7 cells/250 μl buffer (70% methanol) and stored at −80 °C.. Samples with cell counts less than 10^7 werelysed in 250 μl buffer. All cell extracts were processed using solid phase exchange cartridges to separate ZDV/TFV phosphates from parent drug and other anabolites, as described [11, 12]. Phosphate fractions and plasma samples were sent on dry ice for analysis by AMS.

AMS and PK analysis

AMS analyses (see Supplemental Digital Content 1) were conducted at the MIT BEAMS Lab using procedures described elsewhere in detail [13]. PK parameters were derived by noncompartmental analysis using WinNonlin (Pharsight, Sunnyvale, CA) version 5.0.1. The elimination rate constant (k_e) was determined from the natural log-transformed data, using linear regression analysis. Elimination half-life was calculated from the following equation: $t_{1/2}$=In2/K_e. All values below the limit of quantification (BQL) before T_{max} was set at 0; the first BQL value after T_{max} was set at half the BQL value; the rest of BQL readings were not used in the analysis.

Statistical analysis

To compare the PK profiles between the microdose and standard dose regimen, we performed the Wilcoxon signed rank test. The same test was used to determine PK differences in CD4+ cells and PBMCs. A p value <0.05 was considered to be statistically significant. All statistical analyses were performed by SPSS 19.0(IBM, Armonk, NY).

RESULTS

Clinical study

Twelve HIV-seronegative subjects (11 male, 1 female; 8 African Americans and 4 Caucasians), ages 35–55 years old, BMI 20.1–31.5 kg/m^2, were randomized into two arms. All subjects tolerated study procedures without clinically significant adverse events.

Detection of parent drug and intracellular triphosphates

The AMS data were reported as dpm/mL and converted to mass concentrations as previously described [6], based on a drug ratio of 100 μg drug/20 μCi for the microdose phase, and 300.1 mg drug/20 μCi for the standard dose phase. Only AMS analysis was

carried out on these samples because of assay sensitivity limits for LC-MS/MS in the microdose phase, and based on prior comparisons of the accuracy of AMS versus LC-MS/MS, with correlation coefficient of 0.96 and ratio of AMS to LC-MS/MS measurement at 1.03 (90% confidence interval 0.92–1.17) [6].

For ZDV, in all postdose samples for all six subjects, ZDV and ZDV-TP were detectable by AMS. For TFV, TFV-DP was not detectable in the CD4+ cell subset postdose in the microdose regimen for a single subject. For both drugs, predose samples in plasma for the second phase of the study were all below detection limits by AMS. In PBMC's, two subjects in each arm had a higher than LLOQ signal at predose during the second phase of the study, although these concentrations were barely higher than the LLOQ. The normalized carryover from microdose phase were less than 1% of standard dose C_{max} for ZDV-TP, and less than 5% of standard dose C_{max} for TFV-DP in predose samples. LLOQ values were never higher than 0.021 dpm/mL but they varied as a function of instrument condition.

Comparison of plasma PK following a microdose versus a standard therapeutic dose of NRTI's

In the ZDV arm, the concentration-time plot (Figure 1a) shows that the total plasma ^{14}C (including both ^{14}C-ZDV and its major metabolite ^{14}C-ZDV-glucuronide as AMS cannot discriminate between these moieties) was similar comparing the microdose and standard dosing regimens. With our limited sampling time points, T_{max} occurred at 2 hours for all subjects in both dosing regimens. For the microdose regimens, normalized median C_{max} for ZDV equivalent (parent drug plus circulating metabolites) was 0.7-fold lower compared to that of the standard dose (Tables 1 and 2). In all six subjects, calculated C_{max} was lower with the microdose regimen (Wilcoxon signed rank test, p=0.03), while the microdose predicted AUC_{inf} was higher in one subject and lower in five subjects (Wilcoxon signed rank test, p=0.08). Noncompartmental analysis calculated plasma ZDV clearance (CL/F), apparent volume of distribution (Vd/F) and half-life for both microdose and standard dose (Table 1). The ratios of all PK parameters derived from the two dosing regimens were within a factor of two (Table 2), indicating reasonable concordance of ZDV plasma PK as assessed by the microdose and standard dose.

For the TDF arm, ^{14}C signal in plasma is mostly TFV [14, 15]. The concentration-time plot is shown in Figure 1b. With the microdose regimen, normalized plasma TFV concentrations were higher compared to the standard dosing regimen (Figure 1b). The T_{max} for plasma TFV was detected at 4 h for all subjects in both regimens. For the microdose regimen, median normalized C_{max} and AUC_{inf} were 1.5 times higher compared to that of the standard dose. Normalized C_{max} and AUC_{inf} calculated after the microdose were higher in all six subjects (Wilcoxon signed rank test, p=0.03). Noncompartmental analysis showed that all the plasma PK parameters (clearance (CL/F), apparent volume of distribution (Vd/F) and half life ($T_{1/2}$)) were similar in microdose and standard dose regimens, with ratios less than two (Tables 1 and 2).

Comparison of PK of intracellular phosphorylated metabolites following a microdose versus a standard therapeutic dose of NRTI's

Figure 1c and d illustrate the concentration-time plots for ZDV-TP in total PBMC's and isolated CD4+ cells. The T_{max} for intracellular ZDV-TP was observed at 2 hours for all cell types, and the intracellular ^{14}C-ZDV-TP C_{max} and AUC_{inf} were higher with the microdose regimen for all six subjects (p=0.03) for both PBMC and CD4+ cells. In PBMCs, the median ratio of normalized C_{max} for ZDV-TP was 4.5-fold higher (291.9 versus 85.5 fmol/10^6 cells) after the 100 μg microdose versus 300 mg dose of ZDV. In the CD4+ cells, the median normalized C_{max} of intracellular ZDV-TP was 17-fold higher (204.2 versus 15.0 fmol/10^6

cells)after microdosing compared to standarddosing (Table 1 and 2). Noncompartmental analysis indicated that for PBMC's, the AUC_{inf} of intracellular ZDV-TP changed 3.9-fold over the dose range studied (100 μg to 300 mg). In CD4+ cells, the AUC_{inf} of ZDV-TP changed 12.9-fold over the same dose range (Table 2).

For TFV-DP, we observed a plateau between 12 to 72 hours post dose (Figure 2e and f). The T_{max} may be observed at any time point on the plateau, with the median at 24h for PBMC's and 72h for CD4+ cells. The median normalized C_{max} in total PBMC's for TFV-DP was comparable after microdosingversus after the standard dose (13.1 versus 10.4 fmol/10^6 cells, p=0.35). In CD4+ cells, the median normalized C_{max} of intracellular TFV-DP was 1.6-fold higher versus after receiving the standard dose (13.17 versus 5.11 fmol/10^6 cells, p=0.08, Table 1 and 2). In Wilcoxon signed rank test, the normalized intracellular TFV-DP AUC_{inf} was 1.43-fold and 1.28-fold greater with the microdose when compared to the standard dose for PBMC's and CD4+ cells, respectively (p>0.05 for both, Table 2). Half-life estimation based on only two terminal time points was similar between the two dosing regimens.

Comparison of PK of intracellular phosphates in CD4+ cells and PBMC's

Intracellular ZDV-TP concentrations were lower in CD4+ cells (p=0.03) compared to PBMC's in subjects receiving the standard dose regimen, but this difference was smaller and not statistically significant following the microdose regimen (p=0.08, Table 3). The median ratio of the PBMC to CD4+ cell AUC_{inf} was 3.81 (range 2.10–6.37) for the standard dose regimen and 2.00 (range 0.76–3.62) for the microdose regimen (Table 3). Half-life estimation of ZDV-TP was not different for CD4+ cells compared to PBMCs in both dosing regimens (Tables 1 and 3).

In both the microdose regimen and the standard dose regimen, TFV-DP showed a similar PK profile for PBMC's and CD4+ cells (p>0.05 for C_{max}, AUC_{inf}, and t1/2). The median ratio of PBMC's to CD4+ cell AUC_{inf} was 1.04 (range 0.48–2.72) for the microdose regimen and 2.15 (range 0.79–3.55) for the standard dose regimen (Table 3).

In comparing PK parameters calculated after the microdose or standard dosing regimens in this specific target cell subset, CD4+ cells demonstrate the same trend as PBMC's. For ZDV-TP, estimated C_{max} and AUC_{inf} were higher after the microdose compared to the standard dose in both CD4+ cells and total PBMC's. For TFV-DP, no statistically significant difference in TFV-DP PK was observed between the microdose and standard dosing regimens in either CD4+ cells or PBMC's (Tables 1 and 2).

The biphasic elimination of intracellular TFV-DP

Following the standard dosing regimen, intracellular TFV-DP concentrations peaked around 12 hours postdosing, then plateaued between 12–72 hours (Figure 2a). After the plateau, there was a slow elimination phase with an estimated $T_{1/2}$ of 64h and 100h in PBMC and CD4+ cells, respectively, but based on only two terminal timepoints (72 and 168 hours postdosing). This biphasic profile was observed in 5 out of 6 subjects. Figure 2a plots the plasma TFV and intracellular TFV-DP of PBMC after a single dose of 300 mg TDF. The TFV-DP concentration continued to increase even after the TFV concentration in plasma dropped to near background.

Figure 2b illustrates the ratio of absolute molar concentration of extracellular TFV and intracellular TFV-DP (with a volume of 0.4 μl per million cells used to estimate concentration [16, 17]). The molar ratio of plasma to intracellular TFV-DP was around 100-fold at 4 hours post dose, and declined to around 2-fold at 72 hours, then fell below 1.0 at 168 hours. These results indicated that the positive concentration gradient of TFV between plasma and intracellular compartments persisted until 72 hours post dosing.

DISCUSSION

In this study, we examined the PK profile of two NRTI's after microdose and standard therapeutic dosing regimens. For zidovudine, plasma PK showed linearity over a 3000-fold dosing range, but the normalized intracellular ZDV-TP was several folds higher with the microdose compared to the standard dosing regimen. For TFV, the normalized plasma AUC_{inf} was 1.5-times higher with the microdose regimen, possibly indicating higher oral bioavailability, but intracellular TFV-DP PK was linear over the 3000-fold dose range tested. As has been suggested previously, the ability to precisely predict human PK from a microdosing study will vary from molecule to molecule [18–20].

The different results for intracellular ZDV-TP and TFV-DP may reflect the different kinases involved in their phosphorylation pathways. ZDV is phosphorylated sequentially by thymidine kinase, thymidylate kinase, and NDP kinase, with thymidylate kinase acting as a rate-limiting enzyme in this process[21]. An earlier study showed that the phosphorylation of ZDV-MP to ZDV-DP is characterized by a high K_m and low K_{cat}, and that intracellular ZDV-MP concentrations were much lower than the K_m of this enzyme after a 300 mg dose[7]. Since the concentration of ZDV-MP is likely to be far below the K_m with either the standard 300 mg dose or the microdose (100 μg), the rate of conversion of ZDV to ZDV-TP should be similar in either case. However, ZDV-MP has been reported to have a substrate suppression effect on thymidylate kinase [21]. With microdose of ZDV, this suppression might be reversed and the enzyme may become more efficient. This could have contributed to the higher ZDV phosphorylation observed with the microdose regimen.

Tenofovir is phosphorylated by adenylate kinase to TFV-MP, and subsequently phosphorylated by nucleoside diphosphate kinase (NDPK) to TFV-DP. *In vitro* data suggest that this second step can also be accomplished by pyruvate kinase and creatine kinase [22]. With TFV and TFV-MP as substrates, both phosphorylation steps are also characterized by low K_{cat} and high K_m[22, 23]. In other words, phosphorylation is carried out at low velocity and high capacity, which may explain the slow accumulation of TFV-DP in cells and the linearity of PK across the 3000-fold range of doses we evaluated in this study.

Studying phosphorylation in the biological target cell subset in vivo may provide valuable information applicable to future drug use and development. It has been reported that ZDV-TP formation is lower in CD4+ cells than in total PBMCs, while lamivudine triphosphate concentrations are the same amongst different cell types[9]. Here we compared the intracellular phosphorylated concentrations of ZDV and TFV in CD4+ cells versus total unfractionated PBMCs. ZDV-TP concentrations were lower in CD4+ cells in the standard dose regimen, while TFV-DP concentrations were not different in these subsets of cells.

The reason for the different phosphorylation of ZDV in specific cell types is not fully understood, and the result of this study supports the existence of a rate-limiting step, or nonlinear phosphorylation specific to ZDV in CD4+ cells. The difference of ZDV-TP concentrations in CD4+ cells compared to PBMCs was statistically significant with standard dosing (Wilcoxon signed rank test, $p<0.05$), but not with microdosing. The difference in ZDV-TP concentrations after microdose and standard dose regimens was larger in CD4+ cells compared to PBMC's (11.9-fold versus 3.9-fold), unlike TFV-DP (similar concentration ratios in PBMC's and CD4+ cells after the two dosing regimens). These observations further support the existence of a rate-limiting step in the formation of ZDV-TP in CD4+ cells.

AMS analysisof the intracellular concentrations of ZDV-TP and plasma TFV yielded excellent concordance with published data [11, 24–26]. The longer estimated half-life and higher AUC_{inf} of ZDV in plasma in this study was almost certainly because AMS measures

the sum of ZDV and its metabolites, mainly ZDV-glucuronide. For TFV-DP, single dose PK for TFV-DP in PBMC has not been reported in the literature, and all PBMC TFV-DP data were collected from subjects who have reached steady state. It is possible to estimate the steady state C_{ss} based on the PK profile after a single dose if the PK is linear and stationary. If we use $C_{ss}=AUC_{inf}/tau$, the derived mean C_{ss} with 300 mg once daily dose is about 60 fmol/10^6 cells. This derived steady state TFV-DP concentration agrees with that reported in the literature [24,27–29].

We observed a significant plateau phase for intracellular TFV-DP concentrations between 12–72 hours following a single dose, followed by a more conventional but prolonged elimination phase. A prolonged plateau phase suggests balanced formation and elimination of TFV-DP. Estimation of the $T_{1/2}$ of TFV-DP is complicated by this multiphasic elimination, i.e., plateau phase followed by prolonged elimination phase, and this may explain the wide range of elimination half-lives reported *in vitro* (50 h in resting T cells) [8,30] and in patients taking TDF (100–150 h) [28,31]. In our study, intracellular TFV-DP formation appeared to continue as plasma TFV concentrations fell to undetectable levels. A detailed calculation of the absolute ratio of concentrations of intracellular and extracellular TFV found that the positive gradient from outside the cell to inside the cell persisted during the TFV-DP formation and plateau phases and for up to 72 hours post dose (Figure 2b). This suggests that it is not necessary to posit a reservoir or accumulation of intracellular TFV-DP precursors such as TFV or TFV-MP. Recent data also proved little accumulation of TFV or TFV-MP in PBMC's *in vivo*[27]. Our single dose studies allowed demonstration of a hysteresis of TFV-DP formation relative to plasma TFV, and a biphasic elimination profile of TFV-DP elimination. This aspect of TFV-DP PK has not been reported previously in the literature. These findings support the observations of Patterson's study, where TDF-DP concentrations were detectable in rectal and vaginal mucosal homogenates as long as 14 days following a single dose[25].

TDF is widely used for the treatment of HIV infection, and also shows promise in preexposure prophylaxis for HIV infection [32, 33]. Our findings may have potential implications for future prevention studies using TDF. The 12 hour time lag before the beginning of the TFV-DP plateau following a single dose suggests that the first dose of TDF for PrEP may need to be taken at least several hours prior to exposure in order to be effective depending on the effective TFV-DP concentration. On the other hand, the long plateau and slow elimination of TFV-DP indicates that a daily dosing regimen should be quite forgiving of missed doses if used continuously.

For the comparison of microdose and standard dosing regimens, we used a fixed sequence design with paired analysis to compensate for interindividual variability, our study was therefore informative despite the small number of subjects. Carryover of intracellular phosphates from the microdose phase was observed, but in only two subjects in each arm and the amount was too small to significantly influence the results of the standard dose phase. A fixed sequence design has the advantage over a crossover design of avoiding potential consequences of induction or inhibition of drug metabolizing enzymes, transporters, kidney function and other potential drug toxicities that might change PK after a standard dose of ZDV or TDF. AMS may facilitate early development of investigational nucleoside analogs through microdosing, but rate-limited metabolism complicates interpretation of intracellular metabolism with microdosing studies. When rate-limiting steps potentially present, caution should be exercised in extrapolating from microdose to standard dose.

Supplementary Material

Refer to Web version on PubMed Central for supplementary material.

Acknowledgments

Source of Funding:

This study was supported by the Johns Hopkins Institute for Clinical and Translational Research, CTSA grant #UL1-RR025005. C.F. has received salary support from an unrestricted research grant awarded by GlaxoSmithKline to The Johns Hopkins University. C.H. has received research grant awarded by Gilead to the Johns Hopkins University.

We would like to thank Tracy King and Lane Bushman for training in the separation of TFV-DP and ZDV-TP. The authors would also like to thank our research coordinators, Christine Radebaugh and Stephanie Everts, and the volunteers who participated in this study.

References

1. Boddy AV, Sludden J, Griffin MJ, et al. Pharmacokinetic investigation of imatinib using accelerator mass spectrometry in patients with chronic myeloid leukemia. Clin Cancer Res. Jul 15; 2007 13(14):4164–4169. [PubMed: 17634544]
2. Gao L, Li J, Kasserra C, et al. Precision and accuracy in the quantitative analysis of biological samples by accelerator mass spectrometry: application in microdose absolute bioavailability studies. Anal Chem. Jul 15; 2011 83(14):5607–5616. [PubMed: 21627104]
3. Yamane N, Tozuka Z, Kusama M, Maeda K, Ikeda T, Sugiyama Y. Clinical relevance of liquid chromatography tandem mass spectrometry as an analytical method in microdose clinical studies. Pharm Res. Aug; 2011 28(8):1963–1972. [PubMed: 21472491]
4. Lappin G, Kuhnz W, Jochemsen R, et al. Use of microdosing to predict pharmacokinetics at the therapeutic dose: experience with 5 drugs. Clin Pharmacol Ther. Sep; 2006 80(3):203–215. [PubMed: 16952487]
5. Kurihara C. Ethical, legal, and social implications (ELSI) of microdose clinical trials. Adv Drug Deliv Rev. Jun 19; 2011 63(7):503–510. [PubMed: 21251940]
6. Chen J, Garner RC, Lee LS, et al. Accelerator mass spectrometry measurement of intracellular concentrations of active drug metabolites in human target cells in vivo. Clin Pharmacol Ther. Dec; 2010 88(6):796–800. [PubMed: 20981003]
7. Lavie A, Schlichting I, Vetter IR, Konrad M, Reinstein J, Goody RS. The bottleneck in AZT activation. Nat Med. Aug; 1997 3(8):922–924. [PubMed: 9256287]
8. Robbins BL, Srinivas RV, Kim C, Bischofberger N, Fridland A. Anti-human immunodeficiency virus activity and cellular metabolism of a potential prodrug of the acyclic nucleoside phosphonate 9-R-(2-phosphonomethoxypropyl)adenine (PMPA), Bis(isopropyloxymethylcarbonyl)PMPA. Antimicrob Agents Chemother. Mar; 1998 42(3):612–617. [PubMed: 9517941]
9. Anderson PL, Zheng JH, King T, et al. Concentrations of zidovudine- and lamivudine-triphosphate according to cell type in HIV-seronegative adults. Aids. Sep 12; 2007 21(14):1849–1854. [PubMed: 17721092]
10. Louissaint NA, Nimmagadda S, Fuchs EJ, et al. Distribution of cell-free and cell-associated HIV surrogates in the colon after simulated receptive anal intercourse in men who have sex with men. J Acquir Immune Defic Syndr. Jan 1; 2011 59(1):10–17. [PubMed: 21937920]
11. King T, Bushman L, Anderson PL, Delahunty T, Ray M, Fletcher CV. Quantitation of zidovudine triphosphate concentrations from human peripheral blood mononuclear cells by anion exchange solid phase extraction and liquid chromatography-tandem mass spectroscopy; an indirect quantitation methodology. J Chromatogr B Analyt Technol Biomed Life Sci. Feb 2; 2006 831(1–2):248–257.
12. King T, Bushman L, Kiser J, et al. Liquid chromatography-tandem mass spectrometric determination of tenofovir-diphosphate in human peripheral blood mononuclear cells. J Chromatogr B Analyt Technol Biomed Life Sci. Nov 7; 2006 843(2):147–156.

13. Liberman RG, Tannenbaum SR, Hughey BJ, et al. An interface for direct analysis of (14)c in nonvolatile samples by accelerator mass spectrometry. Anal Chem. Jan 15; 2004 76(2):328–334. [PubMed: 14719879]
14. Naesens L, Bischofberger N, Augustijns P, et al. Antiretroviral efficacy and pharmacokinetics of oral bis(isopropyloxycarbonyloxymethyl)-9-(2-phosphonylmethoxypropyl)adenine in mice. Antimicrob Agents Chemother. Jul; 1998 42(7):1568–1573. [PubMed: 9660984]
15. Kearney BP, Flaherty JF, Shah J. Tenofovir disoproxil fumarate: clinical pharmacology and pharmacokinetics. Clin Pharmacokinet. 2004; 43(9):595–612. [PubMed: 15217303]
16. van Kampen JJ, Reedijk ML, Burgers PC, et al. Ultra-fast analysis of plasma and intracellular levels of HIV protease inhibitors in children: a clinical application of MALDI mass spectrometry. PLoS One. 2010; 5(7):e11409. [PubMed: 20625386]
17. Ford J, Khoo SH, Back DJ. The intracellular pharmacology of antiretroviral protease inhibitors. J Antimicrob Chemother. Dec; 2004 54(6):982–990. [PubMed: 15537695]
18. Ieiri I, Nishimura C, Maeda K, et al. Pharmacokinetic and pharmacogenomic profiles of telmisartan after the oral microdose and therapeutic dose. Pharmacogenet Genomics. Aug; 2011 21(8):495–505. [PubMed: 21691256]
19. Maeda K, Takano J, Ikeda Y, et al. Nonlinear pharmacokinetics of oral quinidine and verapamil in healthy subjects: a clinical microdosing study. Clin Pharmacol Ther. Aug; 2011 90(2):263–270. [PubMed: 21716273]
20. Programme(EUMAPP) EMAP. Outcomes from EUMAPP – a study comparing in vitro, in silico, microdose and pharmacological dose pharmacokinetics. http://www.eumapp.com/pdfs/EUMAPP%20SUMMARY.pdf
21. Jorajuria S, Dereuddre-Bosquet N, Becher F, et al. ATP binding cassette multidrug transporters limit the anti-HIV activity of zidovudine and indinavir in infected human macrophages. Antivir Ther. Aug; 2004 9(4):519–528. [PubMed: 15456083]
22. Koch K, Chen Y, Feng JY, et al. Nucleoside diphosphate kinase and the activation of antiviral phosphonate analogs of nucleotides: binding mode and phosphorylation of tenofovir derivatives. Nucleosides Nucleotides Nucleic Acids. Aug; 2009 28(8):776–792. [PubMed: 20183617]
23. Topalis D, Alvarez K, Barral K, et al. Acyclic phosphonate nucleotides and human adenylate kinases: impact of a borano group on alpha-P position. Nucleosides Nucleotides Nucleic Acids. Apr; 2008 27(4):319–331. [PubMed: 18404568]
24. Baheti G, Kiser JJ, Havens PL, Fletcher CV. Plasma and intracellular population pharmacokinetic analysis of tenofovir in HIV-1-infected patients. Antimicrob Agents Chemother. Nov; 2011 55(11):5294–5299. [PubMed: 21896913]
25. Patterson KB, Prince HA, Kraft E, et al. Penetration of Tenofovir and Emtricitabine in Mucosal Tissues: Implications for Prevention of HIV-1 Transmission. Sci Transl Med. Dec 7.2011 3(112): 112re114.
26. Gagnieu MC, Barkil ME, Livrozet JM, et al. Population pharmacokinetics of tenofovir in AIDS patients. J Clin Pharmacol. Nov; 2008 48(11):1282–1288. [PubMed: 18779377]
27. Bushman LR, Kiser JJ, Rower JE, et al. Determination of nucleoside analog mono-, di-, and tri-phosphates in cellular matrix by solid phase extraction and ultra-sensitive LC-MS/MS detection. J Pharm Biomed Anal. Sep 10; 2011 56(2):390–401. [PubMed: 21715120]
28. Hawkins T, Veikley W, St Claire RL 3rd, Guyer B, Clark N, Kearney BP. Intracellular pharmacokinetics of tenofovir diphosphate, carbovir triphosphate, and lamivudine triphosphate in patients receiving triple-nucleoside regimens. J Acquir Immune Defic Syndr. Aug 1; 2005 39(4): 406–411. [PubMed: 16010161]
29. Kiser JJ, Aquilante CL, Anderson PL, King TM, Carten ML, Fletcher CV. Clinical and genetic determinants of intracellular tenofovir diphosphate concentrations in HIV-infected patients. J Acquir Immune Defic Syndr. Mar 1; 2008 47(3):298–303. [PubMed: 18398970]
30. Borroto-Esoda K, Vela JE, Myrick F, Ray AS, Miller MD. In vitro evaluation of the anti-HIV activity and metabolic interactions of tenofovir and emtricitabine. Antivir Ther. 2006; 11(3):377–384. [PubMed: 16759055]

31. Delaney, WEt; Ray, AS.; Yang, H., et al. Intracellular metabolism and in vitro activity of tenofovir against hepatitis B virus. Antimicrob Agents Chemother. Jul; 2006 50(7):2471–2477. [PubMed: 16801428]
32. Abdool Karim Q, Abdool Karim SS, Frohlich JA, et al. Effectiveness and safety of tenofovir gel, an antiretroviral microbicide, for the prevention of HIV infection in women. Science. Sep 3; 2010 329(5996):1168–1174. [PubMed: 20643915]
33. Myers GM, Mayer KH. Oral preexposure anti-HIV prophylaxis for high-risk U.S. populations: current considerations in light of new findings. AIDS Patient Care STDS. Feb; 2011 25(2):63–71. [PubMed: 21284497]

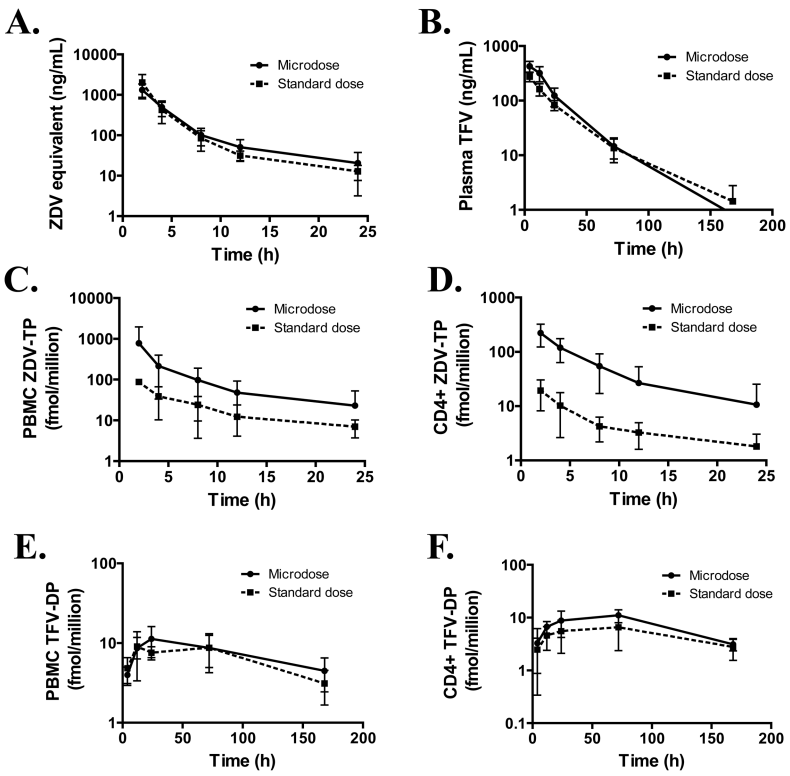

Fig. 1.

Comparison of plasma and intracellular PK after the microdose (100 μg), and standard dose (300 mg) Shown are concentration of ZDV equivalents or TFV in plasma (a,b), and concentration of intracellular ZDV-TP or TFV-DP (c,d,e,f) in the 6 subjects (mean±sd), normalized to a 300 mg dose, versus time. (A) Plasma concentration-time curve for ZDV equivalents (includes ZDV, ZDV-glucuronide and other metabolite of ZDV in plasma) with microdose regimen (circles, solid line) and standard dose regimen (squares, dashed line). (B) Plasma concentration-time curves for TFV with microdose regimen (circles, solid line) and standard dose regimen (squares, dashed line). (C) ZDV-TP concentration-time curve for PBMCs with microdose regimen (circles, solid line) and standard dose regimen (squares, dashed line). (D) ZDV-TP concentration-time curve for CD4+ cells with microdose regimen (circles, solid line) and standard dose regimen (squares, dashed line). (E) TFV-DP concentration-time curve for PBMCs with microdose regimen (circles, solid line) and standard dose regimen (squares, dashed line). (F) TFV-DP concentration-time curve for CD4+ cells with microdose regimen (circles, solid line) and standard dose regimen (squares, dashed line).

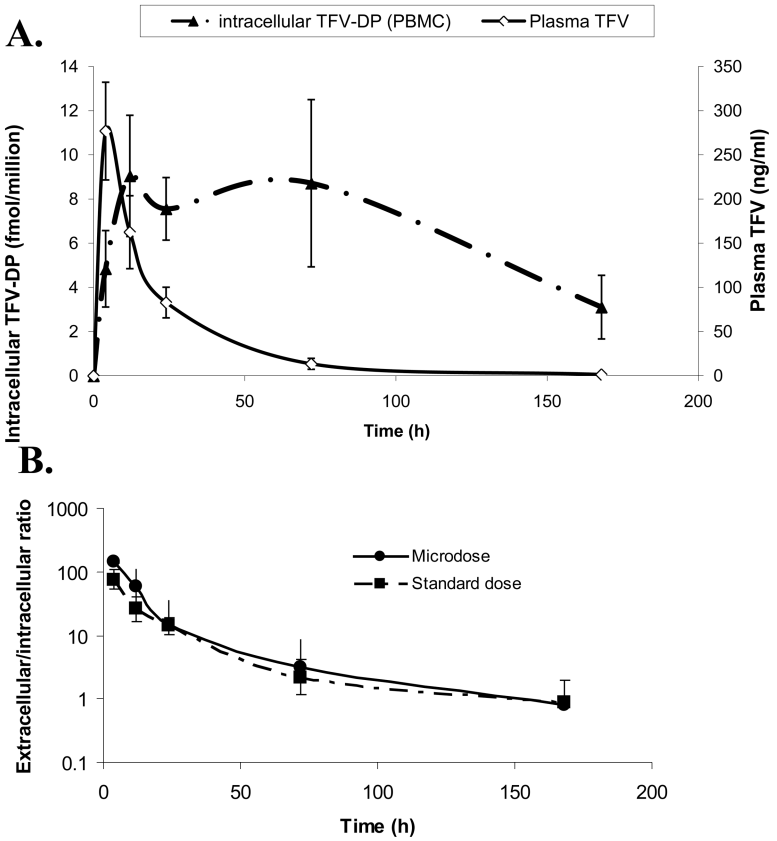

Fig. 2.

Biphasic elimination of TFV-DP after a single dose of TDF. (A) Overall results of PK after a single dose (300mg) of TDF. The solid line represents the plasma TFV concentrations (mean±sd). The dashed line represents the intracellular TFV-DP concentrations (mean±sd). (B) Molar ratio (median ± range) of plasma TFV to intracellular TFV-DP in PBMC over 168h after dose with microdose regimen (circles, solid line) and standard dose regimen (squares, dashed line).

Table 1

PK parameters of ZDV, TFV and their intracellular metabolites ZDV-TP and TFV-DP. All parameters were shown as median (range)

Drug treatment	Sample	$t_{1/2}$ (h)	C_{max} *	T_{max} (h)	$AUC_{0\text{-}inf}$ **	Vd/F (L)	CL/F (L/h)
ZDV 100 μg	Plasma	4.5 (2.3–6.0)	1157.4 (725.1–2130.3)	2	4269.3 (3369.3–8402.7)	364.7 (134.4–605.0)	70.5 (35.7–89.0)
	PBMC	6.6 (4.2–7.7)	291.9 (235.7–3179.8)	2	1836.6 (1072.5–11616.2)	N/A	N/A
	CD4+	4.8 (3.7–9.6)	204.2 (115.4–379.5)	2	1265.8 (609.3–3209.6)	N/A	N/A
ZDV 300 mg	Plasma	4.5 (3.8–4.9)	1414.5 (1117.7–3637.0)	2	4458.8 (3567.1–10855.2)	411.2 (167.9–594.6)	68.2 (27.6–84.1)
	PBMC	6.3 (3.2–17.6)	85.5 (31.9–146.2)	2	577.8 (157.3–1610.4)	N/A	N/A
	CD4+	8.2 (3.8–24.3)	15.0 (10.4–39.8)	2	151.1 (58.7–263.9)	N/A	N/A
TDF 100 μg	Plasma	14.1 (12.3–34.0)	432.0 (287.1–525.0)	4	9658.2 (6057.9–15240.0)	665.7 (477.5–875.7)	31.3 (19.7–49.5
	PBMC	159.0 (61.4–480.4)	13.1 (4.9–17.0)	24 (4–24)	2334.2 (1199.9–4026.4)	N/A	N/A
	CD4+	67.2 (38.1–153.0)	13.2 (6.1–14.1)	72 (24–72)	1925.3 (960.7–2926.4)	N/A	N/A
TDF 300 mg	Plasma	21.4 (14.7–26.3)	257.7 (220.9–375.6)	4	6652.5 (5485.9–8081.2)	1261.2 (850.2–1969.6)	45.6 (37.1–54.7)
	PBMC	63.8 (31.4–185.5)	10.4 (8.6–13.3)	24 (12–72)	1525.9 (837.2–2609.6)	N/A	N/A
	CD4+	99.8 (49.8–284.2)	5.1 (3.8–11.8)	72 (12–72)	1500.0 (534.3–1787.4)	N/A	N/A

* Units of C_{max} are as follows: Plasma (ng/mL), PBMC and CD4+ (fmol/million cells)

** Units of AUC_{inf} are as follows: Plasma (ng*h/mL), PBMC and CD4+ (fmol*h/million cells)

Table 2

PK parameter ratios of microdose regimen to standard dose regimen. Paired analysis, median (range)

Drug treatment	Sample	$t_{1/2}$	C_{max}	$AUC_{0\text{-}inf}$	Vd/F	CL/F
ZDV	Plasma	1.04 (0.48–1.43)	0.70 * (0.54–0.90)	0.90 (0.77–1.11)	1.04 (0.51–1.85)	1.11 (0.90–1.29)
	PBMC	1.02 (0.24–2.04)	4.47 * (1.79–25.17)	3.87 * (1.20–19.34)	N/A	N/A
	CD4+	0.62 (0.20–0.96)	16.97 * (3.43–20.11)	12.90 * (2.41–23.99)	N/A	N/A
TDF	Plasma	0.73 (0.47–1.27)	1.58 * (1.14–1.86)	1.53 * (1.05–2.07)	0.51 * (0.40–0.61)	0.66 * (0.48–0.96)
	PBMC	2.39 (0.44–8.12)	1.12 (0.53–1.64)	1.43 (0.76–4.81)	N/A	N/A
	CD4+	0.76 (0.24–2.77)	1.62 (0.89–3.46)	1.28 (0.96–2.74)	N/A	N/A

* $p<0.05$, Wilcoxon signed rank test.

Table 3

PK parameter ratios of PBMC to CD4+ cells. Paired analysis, median (range)

Drug treatment		$t_{1/2}$	C_{max}	$AUC_{0\text{-}inf}$
ZDV	microdose	1.11 (0.80–1.79)	1.80 (0.89–8.38)	2.00 (0.76–3.62)
	standard dose	0.76 (0.48–0.86)	5.07 * (1.99–12.71)	3.81 * (2.10–6.37)
TDF	microdose	3.14 (0.97–6.28)	1.04 (0.48–2.72)	1.36 (0.76–2.75)
	standard dose	0.84 (0.11–2.98)	2.15 (0.79–3.55)	1.31 (0.85–1.57)

* $p<0.05$, Wilcoxon signed rank test.